Check for updates

Geochemical Baseline and Pre-Mining Environmental Assessment of Heavy Metals at Iron Exploration Area, Northeastern Aswan, Egypt

Mouataz T. Mostafa · Habash El. Nady · Ramadan M. Gomaa ·
Hany F. Abdelgawad · Hassan I. Farhat · Ibrahim H. Khalifa ·
Salman A. Salman

Abstract Wadi Abu Subeira area contains many farms and houses and is one of the promising areas for iron mining. Therefore, 21 surface soil samples were collected and investigated for toxic heavy metals (Pb, Cr, Ni, Cu, Zn, Co, and As) using inductively coupled plasma (ICP) to establish a geochemical baseline for these metals during pre-mining conditions. To decipher the sources of these metals and their interrelationships, multivariate statistical analysis was applied, while to evaluate the degree of pollution and potential environmental risks the environmental indices were used. Abundances of Pb, Cr, Ni, Cu, Zn, Co, and As fluctuated from 17.72 to 0.06, 47.12 to 10.86, 47.88 to 9.25, 45.04 to 6.23, 51.93 to 17.82, 10.55 to 1.24, and 7.04 to 1.66 mg/kg, respectively, displaying a declining trend of Zn > Cr > Ni >
Cu > As > Co > Pb. Additionally, the mean concentrations of all studied metals were found to be significantly lower than the selected international reference standards. Pearson correlation coefficient, principal component analysis, and cluster analysis revealed two geogenic geochemical associations for the studied toxic elements: (1) Zn-As-Ni-Cr-Cu-Co; and (2) Pb. Negative I_{geo} values were observed for all metals, which showed that the samples were uncontaminated and can be considered a geochemical baseline for the study area. Moreover, all CF values were lower than or close to 1, suggesting low contamination levels from all studied metals and supporting the association with natural geological processes. Similarly, Er and RI values of all metals were below 40 and 150, respectively, indicating a low-risk environment. Ultimately, the obtained levels of the studied metals can

M. T. Mostafa · H. E. Nady · R. M. Gomaa ·
H. F. Abdelgawad
Geology Department, Faculty of Science, Arish University, Al Arish 45511, North Sinai, Egypt
e-mail: mouataz.t.mostafa@sci.aru.edu.eg

H. E. Nady
e-mail: dr.habash.elnady@gmail.com

R. M. Gomaa
e-mail: ramgoma2@yahoo.com

H. F. Abdelgawad
e-mail: abdelgawadhany@gmail.com

H. I. Farhat
Geology Department, Faculty of Science, Suez University, Suez 41518, Egypt
e-mail: hassan.farhat@sci.suezuni.edu.eg

I. H. Khalifa
Geology Department, Faculty of Science, Suez Canal University, Ismailia 41522, Egypt
e-mail: ibrahim.kh.2000@gmail.com

S. A. Salman (✉)
Geological Sciences Department, Inorganic Chemical Industries and Mineral Resources Research Division, National Research Centre, 33 El Bohouth St. (Former El Tahrir St.), Dokki, POB 12622, Giza, Egypt
e-mail: sal_man19@yahoo.com; sa.salman@nrc.sci.eg

be used as a geochemical baseline for tracking the future changes in their accumulations in soil sediments considering the current assessment of the area as an environmentally safe area.

Keywords Wadi Abu Subeira · Toxic elements · Geochemical background · Multivariate statistics · Pollution indices

1 Introduction

Numerous studies have reported irreversible damage to ecosystems in the vicinity of active and abandoned ore mines; accordingly, the contamination of mining areas has become an issue of global importance (Boumaza et al., 2021; Shahmoradi et al., 2020). Ecological impacts associated with mining include drastic land disturbances (Diami et al., 2016; Ngugi & Neldner, 2015), deterioration of soil quality (Mazurek et al., 2017), destruction of pre-existing vegetation, and loss of biodiversity (Yang et al., 2014). In addition to being a highly risky and hazardous working environment (Entwistle et al., 2019), mining is associated with many occupational diseases related to metalliferous dust and mining waste, such as silicosis, asbestosis, pneumoconiosis, black lung disease, chronic bronchitis, inflammation, genotoxicity, and target cell death (da Silva-Rêgo et al., 2022). Notably, the different stages of mining, such as extraction, milling, and ore processing, have caused changes in the geochemical distribution of heavy metals, causing perturbations in their cycling and mobilizing them into the environment with concentrations higher than the lithogenic processes (Pereira et al., 2008; Pérez-López et al., 2008). Heavy metals are characterized by high toxicity even at low concentrations, strong resistance to biodegradation, and an ability to form stable compounds with organic matter, carbonates, and iron and manganese oxides in soil particles (Punniyakotti & Ponnusamy, 2018; Ramasamy et al., 2021; Yalcin et al., 2019).

Generally, heavy metals can be derived from natural geochemical processes (e.g., rock weathering, soil formation, volcanic eruption, and atmospheric deposition) and anthropogenic activities (e.g., mining, burning of fossil fuels, industrial emissions, and waste incineration) (Kabir et al., 2021; Kim et al., 2021; Mondal et al., 2018; Turner, 2019).

Noteworthy, anthropogenic sources release metals in more bioaccessible and bioavailable forms compared to those of natural origin (Ekoa Bessa et al., 2021). As a consequence, metals of anthropogenic origin can enter the human body via inhalation (atmospheric dust, aerosols), ingestion (either intended or unintended), and dermal contact, where they accumulate in the human internal tissues or enter the bloodstream (Al-Shidi et al., 2021; Faiz et al., 2009; Lu et al., 2014). In the vicinity of mining areas, especially when there is no vegetation cover, the ingestion pathway becomes of great interest as the bio-geochemical processes accentuate metal mobilization in the environment and encourage migration to groundwater or entering the food chain. Acute short-term metal exposure can cause nausea, vomiting, breathing problems, skin irritation, abdominal discomfort, diarrhea, visual disturbance, headache, and cough (Jayarathne et al., 2018), whereas chronic exposure can affect the central nervous system and cause skeletal damage, kidney dysfunction, disruption of many biochemical processes, and normal functioning of internal organs (Hu et al., 2012).

The term "background" has been defined by the USEPA (2002) as substances or locations that exist in forms not influenced by human activities. The ultimate target for any environmental remediation plan is to restore the natural background or the environmental conditions that dominated before any mining activities (Nordstrom, 2015), which is practically improbable. Furthermore, defining this baseline after the mineralized area witnessed a decades-long history of mining activities (e.g., open pits, waste piles, tailings) is fraught with significant uncertainties, and unfortunately, most environmental impact assessment studies around mining sites were conducted during or after mining. According to Helgen and Moore (1996), trace element levels, mineralogy, and dispersion agents can be used to study sediments under pre-mining conditions. Moreover, there are many other effective geochemical tools, such as the use of stable isotopes, statistical analysis, kinetic modeling, and mass balances, which can also be applied. Particularly, defining the geochemical background values for toxic elements in mineralized but unmined areas (pre-mining conditions) facilitates the planning for risk assessment, monitoring, and remediation plans during and after mining (Nordstrom, 2015). Additionally, calculating the soil pollution indices requires the proper

selection of the geochemical background, which is important to get more acceptable results. Nevertheless, most studies, in the absence of local data or the difficulty of determining it, depend on regional reference standards such as the average elemental contents in the earth's crust of Turekian and Wedepohl (1961). There is an urgent need for setting local backgrounds of element distribution in the different environmental compartments, owing to the variation in geological settings worldwide. This need for determining a natural local geochemical baseline has attracted the attention of several recent studies (e.g., Ahmadi et al., 2018; Dold & Weibel, 2013; Kelepertzis et al., 2012; Romero-Freire et al., 2018; Sababa & Ekoa Bessa, 2022).

Egyptian iron ore deposits are linked with ferruginous sandstones and clays and are considered among Egypt's most economically sustainable resources (Mekkawi et al., 2021). Wadi Abu Subeira, the study area, is located to the northeast of Aswan, South Egypt, and is regarded as a promising developing zone in terms of iron mining and ball clay quarrying, especially with the associated job opportunities for low-income earning inhabitants. Sedimentary iron ores of east Aswan are hosted within the Upper Cretaceous sediments, with iron ores reserves of about 135 million tons (Shaltout et al., 2012) and average iron contents ranging between 46.8% and 85% (Mekkawi et al., 2021), which gives it the potentiality to become one of the major iron mining sites in Egypt. Aswan governorate has historical and economic importance, as it has a global tourism reputation, as well as being one of the agricultural governorates, so a healthy environmental quality must be maintained. The future environmental challenges related to planned mining developments must be assessed since mining impacts can be severe and extend for many kilometers around the mining area. In the short term, the role of mechanical dispersion through water, wind, and topography must be taken into account, especially in seasonal rainy storms (Mokhtari et al., 2018).

At Abu Subeira area, publications covering the geology, lithostratigraphy, origin, mineralizations, and reserves of Aswan iron ores were numerous (Hassan, 2017; Kamh et al., 2022; Meneisy, 2020; Salem & El Gammal, 2015; Soliman et al., 1986; Youssef et al., 2018). However, no geochemical investigations were performed concerning heavy metal levels in the study area, which remains a paucity of evidence about the current environmental condition. Therefore, this study was designed to (a) appraise the concentrations of seven heavy metals (As, Cu, Cr, Co, Ni, Pb, and Zn) in surface soil samples to document them before any mining activities and establish a geochemical baseline, (b) reveal the possible origins of the studied metals and decipher the interrelationships between them according to their geochemical behavior, and (c) detect critical points with higher potential pollution and evaluate the presence of ecological risks in these pre-mining conditions. So, the results of this study provide an adequate natural background, or pre-mining baseline, of environmental contamination before ore exploitation that can be compared to determine the real impact of mining activities in the future. In a wider context, these results can be used as an analogy for metallogenic provinces with similar geologic settings, whether in pre-mining, during mining, or post-mining conditions (e.g., Wadi Abu Aggag, Fig. 1). Besides, these data could help to enhance the sustainability of the mining process by setting up monitoring and remediation programs on a reliable geochemical background with better knowledge about the local geology and the geochemical behavior of elements.

2 Materials and Methods

2.1 Study Area and Geologic Setting

Wadi Abu Subeira is located in southern Egypt, east of the Nile River. Administratively, it belongs to Aswan Governorate, as it is about 35 km away from the governorate's capital and about 900 km away from Egypt's capital (Cairo). It is enclosed between latitudes 24° 12′ 09″ to 24° 14′ 17″ N and longitudes 32° 54′ 58″ to 33° 2′ 54″ E (Fig. 1), covering an area of about 4.5 km^2. About fifteen thousand people are living there, forming small urban clusters, and depending on agriculture (e.g., alfalfa, sorghum, maize, and palm trees) and quarrying (e.g., Aswan ball clay) as sources of income. Wadi Abu Subeira is characterized by a hot and dry climate with storm events in the winter that probably cause flash floods, which may result in house demolition, crop damage, and deaths, considering that the direction of the prevailing wind in Aswan City is mainly towards the North (Abdalla et al., 2011). Regarding the topographic features, the elevation increases from 96 m in the west to 114 m in
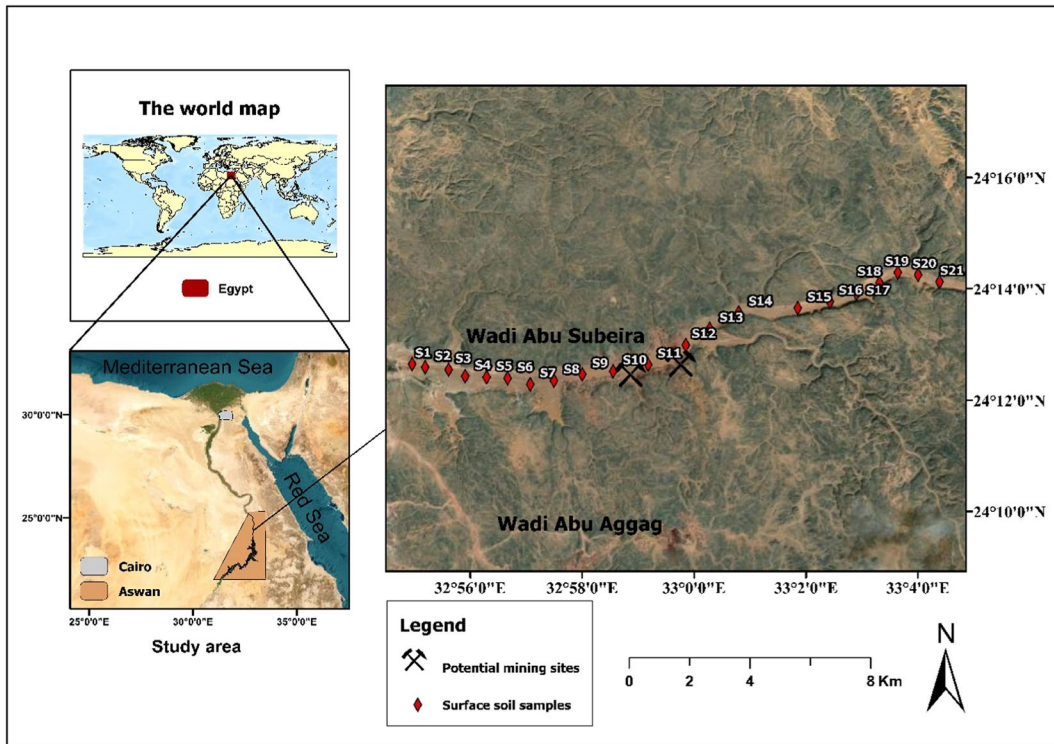
Fig. 1 Location of study area: Wadi Abu Subeira, and surface soil sampling sites

the east, whereas the relief on the flanks of the wadi ranges from 140 m on the southern flank to 180 m on the northern flank, which reflects the uneven topographic relief (Youssef et al., 2018).

The oolitic iron ores are well-distributed in Africa including southern Egypt, northern Sudan, and Nigeria (Hassan, 2017; Mücke, 2000). The iron ore in the study area is hosted within the Upper Cretaceous clastic succession (Nubian Sandstone Series), which lies unconformably on the basement complex of crystalline igneous and metamorphic rocks (Youssef et al., 2018) and includes, from the base upwards, three lithostratigraphic units; the Abu Aggag Formation (Turonian), the Timsah Formation (Coniacian-Santonian) and the Um Barmil Formation (Santonian-Campanian) (Baioumy & Ismael, 2014; Hassan, 2017). These formations are overlaid by Quaternary deposits, which are composed of sandstone and Nile mud, along with Miocene sediments (sandstone and conglomerates). Timsah Formation, the iron-bearing formation, consists of chamosite clayey sandstone alternating with sandy clay, sandstone, ironstone, and iron ore horizons. Concerning the ore body, it reaches a depth of about 80 m (Mekkawi et al., 2021) and is characterized

by an oolitic texture, metallic luster, and red streak. Iron-bearing minerals of Aswan deposits are essentially cryptocrystalline hematite, in addition to the existence of chamosite, and goethite, whereas the gangue minerals are mainly quartz, gypsum, glauconite, pyrite, and clay minerals (Shaltout et al., 2012). Notably, hematite forms tabular and prismatic crystals and sometimes shows growth twinning (Baioumy, 2007).

2.2 Sampling and Field Work

A total of 21 residual surface soil samples (S1-S21) (0–30 cm) were collected, as shown in Fig. 1. Sample locations were planned to avoid areas of anthropogenic influences (e.g., agricultural activities and clay quarrying) in addition to carrying out the fieldwork during August in sunny, windless, and rainless weather to avoid metals leaching and washing. Notably, the iron ore deposits were dominated in the middle of the wadi, and no iron mining activities had been observed at the time of the fieldwork. Sampling was carried out using a stainless steel soil probe, which was washed before each sampling in order to reduce cross-contamination and mildew

growth. To confirm that the sample is representative, five sub-samples within a radius of 1 m were randomly collected, homogenized, and bulked together to form one composite sample (500–1000 g) at each sampling location. A portable geographical positioning system (Garmin eTrex 20 model) was used to record the exact locations of sampling points. All samples were labelled and packed up into self-sealing polyethylene bags to keep them isolated and prevent any adverse effects, then the samples were transported immediately to the laboratory. Before the analysis, samples were first air-dried at room temperature (about 27 °C) for 3 days to reach a constant weight. To obtain a finer texture and remove large stones, plant debris, coarse materials, and pebbles, all dried samples were refined using a 2 mm nylon sieve (10-mesh), as fine sediments have higher ecological risks than the coarser fractions (Wang et al., 2021). Refined samples were then grounded to the powder state and stored in clean polyethylene bags until digestion and subsequent geochemical analysis.

2.3 Digestion and Geochemical Analysis

Microwave digestion systems are a commonly used method for sediment sample digestion (Bourliva et al., 2017; Jiang et al., 2018). Briefly, 0.5 g of homogenized soil sample was weighted and transferred to the PTFE vessels. Subsequently, 9 ml of nitric acid (69%) and 1 ml of H_2O_2 were added to the sample. The vessel was closed completely and then transferred to the microwave, to undergo a temperature-controlled program. After cooling to room temperature, the content of the vessel was transferred to a volumetric flask (25 mL) and diluted with ultrapure water to be ready for analysis by ICP-OES.

Geochemical analysis for investigated heavy metals (Pb, Cr, Ni, Cu, Zn, Co, and As) was performed at the Department of Food Toxicology and Contaminants of the Egyptian National Research Centre using the Agilent 5100 Synchronous Vertical Dual View (SVDV) ICP-OES with Agilent Vapor Generation Accessory (VGA 77). Quality assurance and quality control (QA and QC) included using reagents of high purity, reagent blanks, analytical triplicates, samples submission to the laboratory in random order, and the analysis of standard reference materials from the Merck Company (Germany) and the National Institute of Standards and Technology (NIST). The standard deviations (SD) of replicate samples ranged

between 2 and 9%, and the recovery percentages varied from 88 to 110% for all tested metals. Additionally, the analytical precision was less than 5%.

2.4 Descriptive and Multivariate Statistical Analysis

Metal concentrations were expressed in terms of descriptive statistics, including mean, median, maximum, minimum, coefficient of variation, and standard deviation. Pearson correlation analysis was applied to elucidate the interrelationships between metal pairs and to understand their similarity or dissimilarity regarding their origin and geochemical characteristics. Principle component analysis was applied to eliminate the less significant variables using Varimax rotation (Chenery et al., 2020), and Ward's method was used to employ hierarchical cluster analysis (Patinha et al., 2015). All descriptive and multivariate statistics were conducted using SPSS 23 for Windows and Minitab 17 software packages, whereas the graphical representation of the results was created using Origin 2021 software package.

2.5 Pollution and Ecological Risk Indices

Pollution and ecological indices are effective tools for simplifying raw environmental information for decision makers after processing and analyzing them (Caeiro et al., 2005; Qingjie et al., 2008). Pollution indices can be classified into two main categories: single indices are calculated for each metal individually, and complex indices study sediment contamination in a more integrated way, concerning the content of more than one heavy metal or the sum of individual indices (Qingjie et al., 2008).

Geo-accumulation index (I_{geo}), a widely used individual index, allows the estimation of toxic metals accumulation and the comparison between the present and previous contamination levels regarding a specified background as a reference (Muller, 1969; Shirani et al., 2020; Zhiyuan et al., 2011). I_{geo} is calculated using the following formula (Muller, 1969):

$$\left(I_{geo}\right)_n = \log_2\left(\frac{C_n}{1.5 \times B_n}\right) \tag{1}$$

In Eq. (1), C_n is the measured content of the nth heavy metal in surface soil samples (mg.kg^{-1}), B_n is

Table 1 Basic statistical description of heavy metal concentrations in surface soil samples from Wadi Abu Subeira (mg/kg) and some standard references for comparison

Sites	Pb	Cr	Ni	Cu	Zn	Co	As
S1	0.06	47.12	44.25	45.04	47.67	10.55	7.04
S2	0.39	19.80	14.40	15.59	27.62	ND	2.84
S3	2.95	16.05	13.72	11.19	31.28	ND	3.69
S4	0.91	17.36	17.12	12.76	37.78	ND	3.72
S5	1.17	11.87	12.64	9.83	29.30	ND	1.85
S6	0.32	13.20	10.64	6.23	27.11	ND	1.89
S7	1.29	12.99	10.41	7.28	25.16	ND	3.80
S8	2.63	32.39	25.15	17.01	46.33	2.85	5.71
S9	2.97	16.89	15.17	12.81	37.45	ND	3.89
S10	17.72	14.67	14.68	12.50	37.46	ND	4.72
S11	1.76	19.92	27.33	10.86	44.05	ND	4.79
S12	3.34	26.31	41.64	21.65	49.49	7.76	5.82
S13	4.16	19.81	30.59	11.97	41.39	1.70	4.76
S14	0.85	29.32	47.88	16.98	51.93	6.53	5.60
S15	1.12	13.90	10.45	7.25	20.24	1.45	2.41
S16	1.95	17.65	15.73	11.77	29.07	1.86	2.33
S17	5.21	19.95	17.44	12.38	30.63	1.95	2.93
S18	2.46	19.75	18.14	13.63	30.97	1.36	3.16
S19	2.40	16.52	18.33	16.33	29.77	2.21	3.54
S20	2.68	15.20	13.76	9.15	25.86	1.98	2.96
S21	1.51	10.86	9.25	6.31	17.82	1.24	1.66
Mean	2.75	19.60	20.42	13.74	34.21	3.45	3.77
Median	1.95	17.36	15.73	12.38	30.97	1.97	3.69
Maximum	17.72	47.12	47.88	45.04	51.93	10.55	7.04
Minimum	0.06	10.86	9.25	6.23	17.82	1.24	1.66
SD	3.67	8.35	11.54	8.16	9.67	3.07	1.47
CV	13.45	69.80	133.18	66.62	93.46	9.42	2.16
Turekian and Wedepohl (1961)[a]	20	90	68	45	95	19	13
Taylor (1964)[b]	12.5	100	75	55	70	25	1.8
Wedepohl (1995)[c]	17	35	18.6	14.3	52	11.6	2

[a]Distribution of the elements in Earth's Crust in sedimentary rocks (shales)

[b]Abundance of chemical elements in the Continental Crust (Crustal average)

[c]Chemical composition of the Continental Crust (Upper Continental Crust)

ND not detected, *SD* standard deviation, *CV* coefficient of variation

the level of the nth heavy metal in the background, and the constant (1.5) is a background matrix correction factor, which is used to decrease the possible effect of variability in background values due to natural fluctuations of data and minor anthropogenic influences (Loska et al., 2004; Zhiyuan et al., 2011). The world average elemental contents in the earth's crust, reported by Turekian and Wedepohl (1961), was used as a reference in this study based on element abundances in sedimentary rocks (shale)

(Table 1). Many recent studies depend on this background (e.g., Ghrefat et al., 2011; Kouidri et al., 2016; Mandeng et al., 2019; Singh et al., 2017; Williams & Antoine, 2020). Muller (1969) classified the geo-accumulation index into seven classes to eliminate the impact of lower differentiated results as shown in Table S1.

Contamination factor (CF) is another single-element index, used for assessment of sediments contamination and also it is important in calculating

other complex indices (Sundar et al., 2021). It is the ratio between the individual heavy metal content in the soil sample (C_{sample}) to the reference level (geochemical background) of the particular heavy metal ($C_{background}$) (Hakanson, 1980). The Turekian and Wedepohl (1961) element concentrations for shale were also used as background values, and the equation for CF calculation is as follows:

$$CF = \frac{C_{sample}}{C_{background}} \tag{2}$$

CF results were classified into four categories based on the contamination levels on a scale ranging from 1 to 6 as shown in Table S2.

Pollution load index (PLI), introduced by Tomlinson et al. (1980), investigates the overall pollution risk by combining the impact of all analyzed metals (Varol, 2011). It depends on contamination factor values (CF) as PLI for one site is calculated as the nth root of the product of the multiplications of the individual contamination factor values (Kabir et al., 2021; Liu et al., 2005; Wu et al., 2018) as the following:

$$PLI = \left(CF_1 \times CF_2 \times CF_3 \times \cdots \times CF_n \right)^{\frac{1}{n}} \tag{3}$$

where CF denotes the contamination factor of each heavy metal, while n is the number of analyzed heavy metals, which in this study were seven metals. Notably, PLI values close to one designate no metal pollution (perfect sediment quality), whereas PLI values equal to one indicate that heavy metal loads are close to the background (baseline level of pollution), and PLI values more than unity indicate that the pollution exists (deterioration of sediment quality) (Tomlinson et al., 1980).

In the context of a more comprehensive understanding of the overall pollution level, the contamination degree index (C_{deg}), suggested by Hakanson (1980), was calculated as the sum of CF values for all studied metals (Suryawanshi et al., 2016; Weissmannová & Pavlovský, 2017), which is calculated as follows:

$$C_{deg} = \sum_{i=1}^{n} CF \tag{4}$$

where CF represents contamination factor values, and n is the number of analyzed heavy metals. Hakanson's

(1980) initial scale for categorizing the results C_{deg} was based on a study that included eight analyzed metals. Therefore, this scale is adjusted in studies containing fewer elements, such as this study, as described in Table S3.

Nemerow pollution index (PIN_{emerow}) directly reflects sediment pollution by allowing the assessment of the overall pollution degree with a precious scale (Brady et al., 2014; Qingjie et al., 2008). Additionally, it is compatible with extreme values as it highlights the impact of the most pollution-contributing heavy metal, as shown in the following formula (Hakanson, 1980; Kabir et al., 2021):

$$PI_{Nemerow} = \sqrt{\frac{(CF_{ave})^2 + (CF_{max})^2}{n}} \tag{5}$$

where CF_{ave} is the average value for the contamination factor of all heavy metals, CF_{max} is the maximum value for the contamination factor of all heavy metals, and n is the number of analyzed heavy metals. Furthermore, five classes are used to describe the pollution status according to $PI_{Nemerow}$ index results: safety domain and no pollution status ($PI_{Nemerow} \leq 0.7$), precaution domain and warning limit of pollution ($0.7 < PI_{Nemerow} \leq 1$), slight pollution status ($1 < PI_{Nemerow} \leq 2$), moderate pollution status ($2 < PI_{Nemerow} \leq 3$) and heavy pollution status ($PI_{Nemerow} > 3$) (Hakanson, 1980; Liang et al., 2013; Weissmannová & Pavlovský, 2017; Yesilkanat & Kobya, 2021).

The individual ecological risk factor (Er) was developed in order to integrate the content of heavy metals with their ecological sensitivity and toxicity degree (Guo et al., 2012; Maanan et al., 2015). Er depends on contamination factor values (CF), the toxicity limit of each heavy metal, and the biological response to this toxicity level (Kouchou et al., 2020). After the assessment of the potential risk for each metal individually, the overall ecological risk (RI) caused by the integrated impact of metals should be determined by summing the potential individual risks (Er) (Kowalska et al., 2016; Luo et al., 2007). Hence, individual ecological risk factor Er and overall ecological risk index (RI) can be quantitatively calculated using the following formulas:

$$Er = T_r^i \times CF^i \tag{6}$$

Table 2 Pearson correlation coefficients between heavy metal compositions in surface soil samples from Wadi Abu Subeira

*Correlation is significant at the 0.05 level (two-tailed)

Metals	Pb	Cr	Ni	Cu	Zn	Co
Pb	1.00					
Cr	-0.16	1.00				
Ni	-0.10	0.82[*]	1.00			
Cu	-0.09	0.91[*]	0.72[*]	1.00		
Zn	0.11	0.75[*]	0.88[*]	0.61[*]	1.00	
Co	-0.42	0.85[*]	0.87[*]	0.89[*]	0.75[*]	1.00
As	0.16	0.82[*]	0.84[*]	0.74[*]	0.90[*]	0.83[*]

$$RI = \sum_{i=1}^{n} Er \qquad (7)$$

where Er is the individual ecological risk factor, T_r^i is the toxic-response factor for a specific metal (i), CF^i is the contamination factor of a specific metal (i), RI is the overall ecological risk index and n is the number of measured metals. This study used the biological toxic-response factors proposed by Hakanson (1980) (Table S4). Detailed information regarding the classification of Er and RI results was described in Table S5.

3 Results and Discussion

3.1 Heavy Metals Concentrations and Univariate Statistical Analysis

Geochemical analysis results of heavy metals for surface soil samples along with their fundamental statistical characteristics, including maximum, minimum, mean, median, standard deviation, and coefficient of variation, were presented in Table 1, which exhibited a wide range of concentrations throughout the study area. Correspondingly, abundances of Pb, Cr, Ni, Cu, Zn, Co, and As fluctuated from 17.72 to 0.06, 47.12 to 10.86, 47.88 to 9.25, 45.04 to 6.23, 51.93 to 17.82, 10.55 to 1.24, and 7.04 to 1.66 mg/kg, respectively, with a mean value of 2.75, 19.60, 20.42, 13.74, 34.21, 3.45, and 3.77 mg/kg, respectively. Hence, the selected metals displayed a declining trend of Zn > Cr > Ni > Cu > As > Co > Pb. The coefficient of variation (9.42– 133.18%) obviously indicated an inhomogeneous distribution of the analyzed elements. Noteworthy, the relatively extreme levels of Cr, Cu, Co, and As at (S1) and Ni and Zn at (S14), compared with the median values, pointed out local hotspots enriched with these metals. This variation may be attributed to their derivation through the progressive erosion of different rock types (e.g., basalt and mudstones) and the mixing of different proportions of the weathering products (Hassan, 2017).

Table 3 Results of principle component analysis for heavy metals in surface soil samples from Wadi Abu Subeira

Heavy metals	Principal components	
	PC1	PC2
Pb	-0.145	0.871
Cr	0.413	-0.053
Ni	0.405	0.171
Cu	0.390	-0.188
Zn	0.390	0.347
Co	0.408	-0.144
As	0.417	0.182
Eigenvalues	5.295	1.081
Proportion of variance	75.64%	15.46%
Cumulative % of variance	75.64%	91.10%
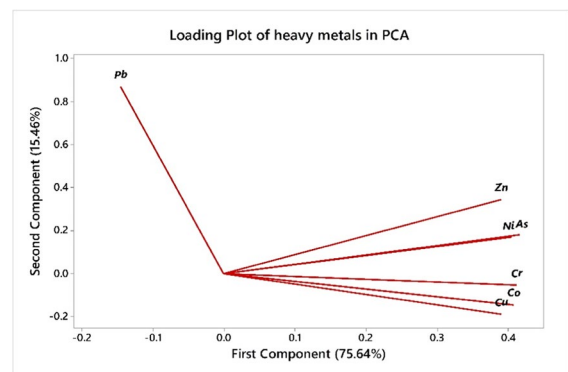
Fig. 2 2D plot of principle component analysis loadings (PC1) and (PC2) for the studied heavy metals in surface soil samples from Wadi Abu Subeira area
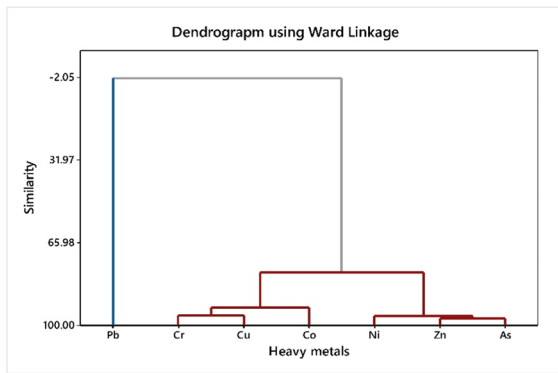
Fig. 3 Similarity dendrogram of the hierarchical cluster analysis for heavy metals in surface soil samples from Wadi Abu Subeira area

The comparison of the studied elements mean with the world reference standards (Table 1) showed that all studied elements were found to be significantly lower than the reference standards reported by Turekian and Wedepohl (1961). Additionally, only the mean value of arsenic was higher than the reference value of Taylor (1964). Nickel, copper, and arsenic mean values were about three times lower than Turekian and Wedepohl's (1961) background values, while Zn mean value was about two times lower than Taylor's (1964) background values. Moreover, in comparison with the upper continental crust values of Wedepohl (1995), it could be observed that the mean values of nickel and arsenic were higher than this standard, whereas the copper mean value was close to the corresponding value.

Given the low proportions of analyzed metals, which were much lower than the international standards, it was very likely that metal enrichment would be in its natural state and was attributed to the chemical weathering of the surrounding rocks with no anthropogenic inputs. Therefore, geochemical processes and local lithology appeared to play a key role in controlling the concentrations of elements. A similar finding was reported by Kelepertzis et al. (2012), who stated that metal contents in surface water and stream sediments were attributed to the chemical weathering of the sulfide minerals of Chalkidiki ore deposits, a pre-mining area in Greece. In the same way, Dabiri et al. (2017) found that the release of nickel, chromium, lead, and zinc into the soil, in a

mineralized area in Iran, was related to the chemical weathering and alteration of basalt, andesite-basalt, and ignimbrite rocks.

The geology of the study area is dominantly composed of outcropping Precambrian basement rocks, overlying by the Upper Cretaceous Nubian Sandstone (Meneisy, 2020). The basement rocks (peneplained crystalline igneous and metamorphic rocks) were mainly represented by schists, gneisses, and highly fractured hills of coarse-grained Aswan granite (Baioumy & Ismael, 2014; Kamh et al., 2022) and basalts of Wadi Natash (Bernau et al., 1987).

As a consequence, Zn and Pb could be mainly associated with the erosion and fragmentation of gneisses (Sababa & Ekoa Bessa, 2022), as the oolitic iron ore at Abu Subeira contains 6.1 – 136.7 and 5.1 – 79.1 mg/kg of Pb and Zn, respectively, whereas Cr is known to occur in trace concentrations in basaltic rocks, so it may have resulted from the weathering of the Timsah and Um Barmil formations in the study area, which contain Cr up to 160 and 112 mg/kg, respectively (Hassan, 2017). On the other hand, the iron-bearing minerals hosted in the mineralizations of the Upper Cretaceous clastic succession were mainly hematite, chamosite, and goethite, in addition to the presence of pyrite and siderite (Shaltout et al., 2012). Hence, Cu could be related to the sulfide minerals like pyrite that accompany the iron ore deposits (Dabiri et al., 2017) or the mineralized porphyry Cu in the Eastern Desert (Ahmed & Gharib, 2016). Likewise, iron-bearing minerals (e.g., hematite and goethite) can be regarded as the major source of Co due to the isomorphous substitution of Fe with Co, and in a similar way, arsenic is also recognized to be associated with the iron ore deposit (Taylor, 1968). Taylor (1971) stated a similar association of Cu and As with the iron ore body in the Pahang mine in Malaysia.

3.2 Inter-Elemental Relationships and Geochemical Behavior

Pearson correlation analysis was performed between all variables to identify heavy metal sources and their interrelationships. Nearly all metals showed significant positive correlations with each other; conversely, Pb did not show any significant correlation with any of the variables. The strongest correlations

Table 4 Geoaccumulation index values (Igeo) for heavy metals in surface soil samples from Wadi Abu Subeira

Sites	Geoaccumulation index (I_{geo})						
	Pb	Cr	Ni	Cu	Zn	Co	As
S1	-8.97	-1.52	-1.20	-0.58	-1.58	-1.43	-1.47
S2	-6.27	-2.77	-2.82	-2.11	-2.37	NC	-2.78
S3	-3.35	-3.07	-2.89	-2.59	-2.19	NC	-2.40
S4	-5.04	-2.96	-2.57	-2.40	-1.92	NC	-2.39
S5	-4.68	-3.51	-3.01	-2.78	-2.28	NC	-3.40
S6	-6.55	-3.35	-3.26	-3.44	-2.39	NC	-3.37
S7	-4.54	-3.38	-3.29	-3.21	-2.50	NC	-2.36
S8	-3.51	-2.06	-2.02	-1.99	-1.62	-3.32	-1.77
S9	-3.34	-3.00	-2.75	-2.40	-1.93	NC	-2.33
S10	-0.76	-3.20	-2.80	-2.43	-1.93	NC	-2.05
S11	-4.09	-2.76	-1.90	-2.64	-1.69	NC	-2.03
S12	-3.17	-2.36	-1.29	-1.64	-1.53	-1.88	-1.74
S13	-2.85	-2.77	-1.74	-2.50	-1.78	-4.07	-2.03
S14	-5.14	-2.20	-1.09	-1.99	-1.46	-2.13	-1.80
S15	-4.74	-3.28	-3.29	-3.22	-2.82	-4.30	-3.02
S16	-3.94	-2.94	-2.70	-2.52	-2.29	-3.94	-3.07
S17	-2.53	-2.76	-2.55	-2.45	-2.22	-3.87	-2.73
S18	-3.61	-2.77	-2.49	-2.31	-2.20	-4.39	-2.63
S19	-3.64	-3.03	-2.48	-2.05	-2.26	-3.69	-2.46
S20	-3.48	-3.15	-2.89	-2.88	-2.46	-3.85	-2.72
S21	-4.31	-3.64	-3.46	-3.42	-3.00	-4.52	-3.55
Mean	-4.21	-2.88	-2.50	-2.45	-2.11	-3.45	-2.48
Maximum	-0.76	-1.52	-1.09	-0.58	-1.46	-1.43	-1.47
Minimum	-8.97	-3.64	-3.46	-3.44	-3.00	-4.52	-3.55
SD	1.67	0.51	0.70	0.64	0.42	1.05	0.58

SD standard deviation, *NC* not calculated

were between Cu and Cr (r = 0.91) and As and Zn (r = 0.90), at a 0.05 significance level (Table 2). These high correlations indicated similar input sources and exhibit mutual dependencies between heavy metals (Bramha et al., 2014; Fan et al., 2022), whereas the low and negative correlations between Pb and all other metals returned to its different geochemical behavior (e.g., immobility and strongly hydrophobic nature) (Ameh et al., 2016; Liu et al., 2019).

Factors with eigenvalues greater than 1.0 were extracted (Malakootian et al., 2021), which led to a reduction of the initial dataset to two components, explaining a total of 91.10% of data variance (Table 3, Fig. 2). Component 1, with an eigenvalue of 5.30, represented 75.64% of the total variance, and was highly loaded with Cr, Ni, Cu, Zn, Co, and As, while

the second component (PC2), dominated only by Pb, accounts for 15.46% of the total variance. Metals with high positive loadings in component 1 revealed that all these metals originated from an identical source and could be attributed to the lithological origin (the weathered Precambrian basement rocks and Upper Cretaceous clastic succession); in contrast, Pb (component 2) may suggest different geochemical characters. In consistency with Pearson correlation analysis and PCA, hierarchical cluster analysis produced a dendrogram with two main clusters: (1) Zn-As-Ni-Cr-Cu-Co; and (2) Pb. The first cluster was subdivided into three sub-clusters, as highlighted in Fig. 3. The strongest observed association (similarity > 97%) was between zinc and arsenic. These strong associations between the elements in the first cluster reflected their

Table 5 Contamination factor (CF) and contamination degree (Cdeg) values for heavy metals in surface soil samples from Wadi Abu Subeira

Sites	Contamination factor (CF)							C_{deg}
	Pb	Cr	Ni	Cu	Zn	Co	As	
S1	0.003	0.524	0.651	1.001	0.502	0.555	0.542	3.777
S2	0.020	0.220	0.212	0.346	0.291	NC	0.218	1.307
S3	0.148	0.178	0.202	0.249	0.329	NC	0.284	1.389
S4	0.046	0.193	0.252	0.284	0.398	NC	0.286	1.458
S5	0.059	0.132	0.186	0.218	0.308	NC	0.142	1.045
S6	0.016	0.147	0.156	0.138	0.285	NC	0.145	0.888
S7	0.065	0.144	0.153	0.162	0.265	NC	0.292	1.081
S8	0.132	0.360	0.370	0.378	0.488	0.150	0.439	2.316
S9	0.149	0.188	0.223	0.285	0.394	NC	0.299	1.537
S10	0.886	0.163	0.216	0.278	0.394	NC	0.363	2.300
S11	0.088	0.221	0.402	0.241	0.464	NC	0.368	1.785
S12	0.167	0.292	0.612	0.481	0.521	0.408	0.448	2.930
S13	0.208	0.220	0.450	0.266	0.436	0.089	0.366	2.035
S14	0.043	0.326	0.704	0.377	0.547	0.344	0.431	2.771
S15	0.056	0.154	0.154	0.161	0.213	0.076	0.185	1.000
S16	0.098	0.196	0.231	0.262	0.306	0.098	0.179	1.370
S17	0.261	0.222	0.256	0.275	0.322	0.103	0.225	1.664
S18	0.123	0.219	0.267	0.303	0.326	0.072	0.243	1.553
S19	0.120	0.184	0.270	0.363	0.313	0.116	0.272	1.638
S20	0.134	0.169	0.202	0.203	0.272	0.104	0.228	1.313
S21	0.076	0.121	0.136	0.140	0.188	0.065	0.128	0.853
Mean	0.14	0.22	0.30	0.31	0.36	0.18	0.29	1.71
Maximum	0.886	0.524	0.704	1.001	0.547	0.555	0.542	3.777
Minimum	0.003	0.121	0.136	0.138	0.188	0.065	0.128	0.853
SD	0.183	0.093	0.170	0.181	0.102	0.161	0.113	0.746

SD standard deviation, *NC* not calculated

simultaneous release and association with crustal matter (Jianhua et al., 2006; Jose & Srimuruganandam, 2020; Viana et al., 2008).

Generally, the geochemical behavior of heavy metals in the environment can be described in terms of mobility, bioavailability, and bioaccessibility, which are affected by the adsorption of heavy metals on sediment grains (Chen et al., 2016). Earlier studies showed that metal oxides (iron and manganese), carbonates, and organic materials are the most effective sorbents for these metals (Perret et al., 2000; Wang & Li, 2011), as they are capable of developing stable complexes with heavy metals (Fdez-Ortiz de Vallejuelo et al., 2017; Yalcin et al., 2019). In particular, clay minerals are considered the essential reactive components in soil and surface

sediments, having a great influence on metal contents and mobility due to their high cation exchange capacity and affinity (Proust et al., 2013; Suresh et al., 2012). In Wadi Abu Subeira, the Timsah Formation includes three highly plastic clay beds, known as ball clay, that occur as massive gray, yellowish gray, or reddish to brownish gray clays. These beds, with a large reserve of about 10 million metric tons (Baioumy & Ismael, 2014), have great industrial and economic value and can be used in domestic ceramic and tile industries. Moreover, Abu Aggag Formation starts at base with a kaolinitic conglomeratic bed and also contains kaolinitic sandstones (Hassan, 2017). Mineralogically, ball clay is composed of weakly crystalline kaolinite (39–60 wt.%), in addition to tiny amounts of illite (10–19 wt.%) and/or smectite (Baioumy
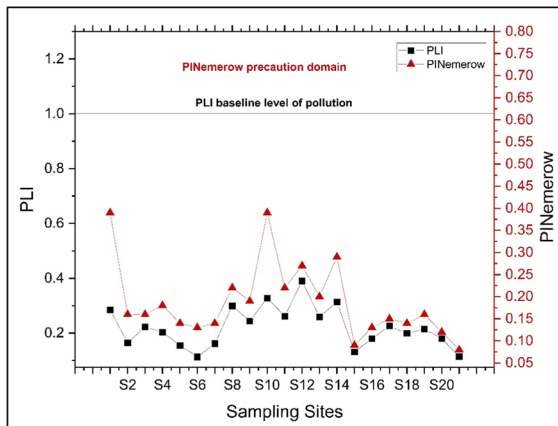
Fig. 4 Results of Nemerow pollution index (PINemerow) and pollution load index (PLI) for heavy metals in surface soil samples from Wadi Abu Subeira area (values below detection limits were not included in the calculation)

& Ismael, 2014; Kamh et al., 2022). Altogether, there is a potential for an association between heavy metals and clay minerals. This agrees with Baioumy et al. (2012), who indicated the association between Cr, Nb, and Zr in the Carboniferous and Cretaceous sedimentary kaolin deposits. Another suggestion is that iron oxides (e.g., hematite and goethite) play a significant role in scavenging toxic metals due to their large capacity for sorption or co-precipitation with them and strong surface reactivity (Shen et al., 2020; Zhao et al., 2021). Furthermore, iron oxides can transport sequestered metals to great distances (Ameh et al., 2016). The strong affinity of nickel and cobalt for iron hydroxides supports this hypothesis (Ekoa Bessa et al., 2021; Kelepertzis et al., 2012).

3.3 Environmental Pollution and Ecological Risk Assessment

Negative I_{geo} values were observed for all metals (Table 4), which showed that the sediments were uncontaminated and can be considered background values (Bramha et al., 2014). The CF ranges of Pb, Cr, Ni, Cu, Zn, Co, and As were 0.003–0.89, 0.12–0.52, 0.14–0.70, 0.14–1.00, 0.19–0.55, 0.07–0.56, and 0.13–0.54, respectively, with mean values of 0.14, 0.22, 0.30, 0.31, 0.36, 0.18, and 0.29, respectively (Table 5). Hence, all CF values were lower than or close to 1.0, suggesting low contamination levels from all studied metals and supporting the association with natural geological processes. C_{deg} values were lower

than 6.0 over all studied sites, depicting low contamination degree, while PLI values ranged from 0.11 at (S6) to 0.39 at (S12) with an average of 0.22, which designated no metal pollution (PLI < 1) (Fig. 4). In the same context, $PI_{Nemerow}$ values were less than 0.7, regardless of the sampling site, which revealed that sediments were in the safety domain (no pollution status) (Fig. 4). As shown in Table 6, Er and RI values of all metals were below 40 and 150, respectively, which indicated a low-risk environment due to heavy metal contaminants, either individually or in combination. In general, the results of individual pollution indices (I_{geo} and CF), overall pollution indices (C_{deg}, PLI, and $PI_{Nemerow}$), and ecological risk indices (Er and RI) were consistent, homogenous, and unanimous that Wadi Abu Subeira was classified as an unpolluted area with nearly no anthropogenic influences.

Despite this low contamination grade, the influence of the planned mining development in the area may be associated with a high potential for the dispersion and remobilization of heavy metals from indigenous rocks into the environment (Romero-Freire et al., 2018; Sababa & Ekoa Bessa, 2022). Mokhtari et al. (2018) reported a dispersion with a mechanical movement for heavy metals around 4 km from a mine site in Iran. In Wadi Abu Subeira, one of the important dispersion agents is the storm events that cause flash floods, which could lead to the free movement of the toxic elements, produce a distinct geochemical signature with ultimate distribution, modify the geomorphic systems, and alter the geochemistry of watersheds (Baeten et al., 2018; Moore & Langner, 2012). Regarding planned mining processes, the impact of dewatering processes and mine waste leaching on groundwater quality (Jahanshahi & Zare, 2015), particularly with the fact that Wadi Abu-Subeira flows westward to meet the Nile River Valley, should not be neglected. Thus, these factors should be considered in order to mitigate the future impacts of heavy metals, which have the ability to form chemically unstable compounds when exposed to the atmosphere after excavation (Diami et al., 2016) and to migrate over long distances in air without declining with time (Mazurek et al., 2017; Pellinen et al., 2021).

Once the mining activity started, regular monitoring is recommended for heavy metal levels in different environmental matrices such as groundwater, soil, and crops, which would allow early evaluation of the potential ecological and human health risks in addition to understanding the behavior and dynamics of metals and their

Table 6 Ecological risks results for heavy metals in surface soil samples from Wadi Abu Subeira

Sites	Individual ecological risk factor (Er)							Overall ecological risk index (RI)
	Pb	Cr	Ni	Cu	Zn	Co	As	
S1	0.02	1.05	3.25	5.00	0.50	2.78	5.42	18.01
S2	0.10	0.44	1.06	1.73	0.29	NC	2.18	5.80
S3	0.74	0.36	1.01	1.24	0.33	NC	2.84	6.51
S4	0.23	0.39	1.26	1.42	0.40	NC	2.86	6.55
S5	0.29	0.26	0.93	1.09	0.31	NC	1.42	4.31
S6	0.08	0.29	0.78	0.69	0.29	NC	1.45	3.59
S7	0.32	0.29	0.77	0.81	0.26	NC	2.92	5.37
S8	0.66	0.72	1.85	1.89	0.49	0.75	4.39	10.75
S9	0.74	0.38	1.12	1.42	0.39	NC	2.99	7.04
S10	4.43	0.33	1.08	1.39	0.39	NC	3.63	11.25
S11	0.44	0.44	2.01	1.21	0.46	NC	3.68	8.25
S12	0.84	0.58	3.06	2.41	0.52	2.04	4.48	13.93
S13	1.04	0.44	2.25	1.33	0.44	0.45	3.66	9.60
S14	0.21	0.65	3.52	1.89	0.55	1.72	4.31	12.84
S15	0.28	0.31	0.77	0.81	0.21	0.38	1.85	4.61
S16	0.49	0.39	1.16	1.31	0.31	0.49	1.79	5.93
S17	1.30	0.44	1.28	1.38	0.32	0.51	2.25	7.49
S18	0.62	0.44	1.33	1.51	0.33	0.36	2.43	7.02
S19	0.60	0.37	1.35	1.81	0.31	0.58	2.72	7.75
S20	0.67	0.34	1.01	1.02	0.27	0.52	2.28	6.11
S21	0.38	0.24	0.68	0.70	0.19	0.33	1.28	3.79
Mean	0.69	0.44	1.50	1.53	0.36	0.91	2.90	7.93
Maximum	4.43	1.05	3.52	5.00	0.55	2.78	5.42	18.01
Minimum	0.02	0.24	0.68	0.69	0.19	0.33	1.28	3.59
SD	0.92	0.19	0.85	0.91	0.10	0.81	1.13	3.66

SD standard deviation, *NC* not calculated

cycling after release into the environment. Future studies about the total organic matter, sediments characteristics, and metals bioavailability are also required. In the same context, mining companies should strive to implement precautionary measures, increasing vegetation coverage, establishing buffer zones to eradicate contamination extension, and using sustainable mining methods. Furthermore, administrators and decision makers should enforce environmental laws and create public awareness about mining impacts.

4 Conclusions

A field survey was conducted to investigate the pre-mining conditions for the mineralized but unmined area of Wadi Abu Subeira, considering heavy metal contaminants in 21 surface soil samples to determine the geochemical background and the elemental associations of heavy metals and document the contamination status before the planned mining development in the area. The geometric means of Pb, Cr, Ni, Cu, Zn, Co, and As were 2.75, 19.60, 20.42, 13.74, 34.21, 3.45, and 3.77 mg/kg, respectively. Nearly all metals showed significant positive correlations with each other except Pb, which did not show any significant correlation with all variables, suggesting that all these metals originated from an identical source (lithological origin); nevertheless, Pb may reveal different geochemical characteristics, which were confirmed by principal component analysis and cluster analysis. The results of individual indices (I_{geo} and CF), overall indices (C_{deg}, PLI, and $PI_{Nemerow}$), and ecological

risk indices (Er and RI) were unanimous that Wadi Abu Subeira was classified as an unpolluted area with nearly no anthropogenic influences, and the dominant sources for heavy metals in the study area were attributed to the natural geochemical processes and local lithology, especially the weathering and decomposition of the Precambrian basement rocks and Upper Cretaceous clastic succession. According to the local geology of the study area, it was suggested that iron oxides (e.g., hematite and goethite) and clay minerals (e.g., kaolinite and illite) had a significant role in scavenging toxic metals. Taken together, study results can serve as a geochemical baseline of environmental contamination for ongoing mining activities, which will help mining companies achieve more sustainable mining by eradicating the contamination extent and setting up knowledge-based monitoring and remediation plans.

Author Statement   **Mouataz T. Mostafa:** Conceptualization, Writing—original draft. **Habash El. Nady:** Visualization, Supervision. **Ramadan M. Gomaa:** Methodology, Formal analysis. **Hany F. Abdelgawad:** Investigation, Methodology. **Hassan I. Farhat:** Investigation, Writing—original draft. **Ibrahim H. Khalifa:** Conceptualization, Software. **Salman A. Salman:** Writing—review & editing, Supervision.

Data Availability   All data generated or analyzed during this study are included in this published article.

Declarations

References

Abdalla, E.-S.M., Enieb, M., & Mohamed, R. N. A. E. (2011). Investigation in selecting the optimum airport runway orientation with special reference to Egyptian airports. *JES Journal of Engineering Sciences, 39*(6), 1261–1280.

Ahmadi, S., Jahanshahi, R., Moeini, V., & Mali, S. (2018). Assessment of hydrochemistry and heavy metals pollution in the groundwater of Ardestan mineral exploration area, Iran. *Environmental Earth Sciences, 77*(5), 212. https://doi.org/10.1007/s12665-018-7393-7

Ahmed, A. H., & Gharib, M. E. (2016). Porphyry Cu mineralization in the eastern desert of Egypt: Inference from geochemistry, alteration zones, and ore mineralogy. *Arabian Journal of Geosciences, 9*(3), 179. https://doi.org/10.1007/s12517-015-2107-x

Al-Shidi, H. K., Sulaiman, H., Al-Reasi, H. A., Jamil, F., & Aslam, M. (2021). Human and ecological risk assessment of heavy metals in different particle sizes of road dust in Muscat, Oman. *Environmental Science and Pollution Research, 28*(26), 33980–33993. https://doi.org/10.1007/s11356-020-09319-6

Ameh, E. G., Kolawole, M. S., Idakwo, S. O., Ameh, C. O., & GabrielImeokparia, E. (2016). Distributional Coefficients and Enrichment Studies of Potentially Toxic Heavy Metals in Soils Around Itakpe Iron-Ore Mine, North Central Nigeria. *Earth Science Research, 6*(1), 85. https://doi.org/10.5539/esr.v6n1p85

Baeten, J., Langston, N., & Lafreniere, D. (2018). A spatial evaluation of historic iron mining impacts on current impaired waters in Lake Superior's Mesabi Range. *Ambio, 47*(2), 231–244. https://doi.org/10.1007/s13280-017-0948-0

Baioumy, H. M. (2007). Iron–phosphorus relationship in the iron and phosphorite ores of Egypt. *Geochemistry, 67*(3), 229–239. https://doi.org/10.1016/j.chemer.2004.10.002

Baioumy, H. M., & Ismael, I. S. (2014). Composition, origin and industrial suitability of the Aswan ball clays, Egypt. *Applied Clay Science, 102*, 202–212. https://doi.org/10.1016/j.clay.2014.09.041

Baioumy, H. M., Gilg, H. A., & Taubald, H. (2012). Mineralogy and Geochemistry of the Sedimentary Kaolin Deposits From Sinai, Egypt: Implications for Control by the Source Rocks. *Clays and Clay Minerals, 60*(6), 633–654. https://doi.org/10.1346/CCMN.2012.0600608

Bernau, R., Darbyshire, D. P. F., Franz, G., Harms, U., Huth, A., Mansour, N., Pasteels, P., & Schandelmeier, H. (1987). Petrology, geochemistry and structural development of the Bir Safsaf-Aswan uplift, Southern Egypt. *Journal of African Earth Sciences (1983), 6*(1), 79–90. https://doi.org/10.1016/0899-5362(87)90109-6

Boumaza, B., Kechiched, R., & Chekushina, T. V. (2021). Trace metal elements in phosphate rock wastes from the Djebel Onk mining area (Tébessa, eastern Algeria): A geochemical study and environmental implications. *Applied Geochemistry, 127*, 104910. https://doi.org/10.1016/j.apgeochem.2021.104910

Bourliva, A., Christophoridis, C., Papadopoulou, L., Giouri, K., Papadopoulos, A., Mitsika, E., & Fytianos, K. (2017). Characterization, heavy metal content and health risk assessment of urban road dusts from the historic center of the city of Thessaloniki, Greece. *Environmental Geochemistry and Health, 39*(3), 611–634. https://doi.org/10.1007/s10653-016-9836-y

Brady, J. P., Ayoko, G. A., Martens, W. N., & Goonetilleke, A. (2014). Enrichment, distribution and sources of heavy metals in the sediments of Deception Bay, Queensland, Australia. *Marine Pollution Bulletin, 81*(1), 248–255. https://doi.org/10.1016/j.marpolbul.2014.01.031

Bramha, S. N., Mohanty, A. K., Satpathy, K. K., Kanagasabapathy, K. V., Panigrahi, S., Samantara, M. K., & Prasad, M. V. R. (2014). Heavy metal content in the beach sediment with respect to contamination levels and sediment quality guidelines: A study at Kalpakkam coast, southeast coast of India. *Environmental Earth Sciences, 72*(11), 4463–4472. https://doi.org/10.1007/s12665-014-3346-y

Caeiro, S., Costa, M. H., Ramos, T. B., Fernandes, F., Silveira, N., Coimbra, A., Medeiros, G., & Painho, M. (2005). Assessing heavy metal contamination in Sado Estuary sediment: An index analysis approach. *Ecological Indicators, 5*(2), 151–169. https://doi.org/10.1016/j.ecolind.2005.02.001

Chen, Y.-M., Gao, J., Yuan, Y.-Q., Ma, J., & Yu, S. (2016). Relationship between heavy metal contents and clay mineral properties in surface sediments: Implications for metal pollution assessment. *Continental Shelf Research, 124*, 125–133. https://doi.org/10.1016/j.csr.2016.06.002

Chenery, S. R. N., Sarkar, S. K., Chatterjee, M., Marriott, A. L., & Watts, M. J. (2020). Heavy metals in urban road dusts from Kolkata and Bengaluru, India: Implications for human health. *Environmental Geochemistry and Health, 42*(9), 2627–2643. https://doi.org/10.1007/s10653-019-00467-4

da Silva-Rêgo, L. L., de Almeida, L. A., & Gasparotto, J. (2022). Toxicological effects of mining hazard elements. *Energy Geoscience, 3*(3), 255–262. https://doi.org/10.1016/j.engeos.2022.03.003

Dabiri, R., Bakhshi Mazdeh, M., & Mollai, H. (2017). Heavy metal pollution and identification of their sources in soil over Sangan iron-mining region, NE Iran. *Journal of Mining and Environment*, 8(2). https://doi.org/10.22044/jme.2016.820

Diami, S. M., Kusin, F. M., & Madzin, Z. (2016). Potential ecological and human health risks of heavy metals in surface soils associated with iron ore mining in Pahang, Malaysia. *Environmental Science and Pollution Research, 23*(20), 21086–21097. https://doi.org/10.1007/s11356-016-7314-9

Dold, B., & Weibel, L. (2013). Biogeometallurgical pre-mining characterization of ore deposits: An approach to increase sustainability in the mining process. *Environmental Science and Pollution Research, 20*(11), 7777–7786. https://doi.org/10.1007/s11356-013-1681-2

Ekoa Bessa, A. Z., Ngueutchoua, G., Kwewouo Janpou, A., El-Amier, Y. A., Njike Njome Mbella Nguetnga, O.-A., Kankeu Kayou, U. R., Bisse, S. B., Ngo Mapuna, E. C., & Armstrong-Altrin, J. S. (2021). Heavy metal contamination and its ecological risks in the beach sediments along the Atlantic Ocean (Limbe coastal fringes, Cameroon). *Earth Systems and Environment, 5*(2), 433–444. https://doi.org/10.1007/s41748-020-00167-5

Entwistle, J. A., Hursthouse, A. S., Marinho Reis, P. A., & Stewart, A. G. (2019). Metalliferous Mine Dust: Human Health Impacts and the Potential Determinants of Disease in Mining Communities. *Current Pollution Reports, 5*(3), 67–83. https://doi.org/10.1007/s40726-019-00108-5

Faiz, Y., Tufail, M., Javed, M. T., Chaudhry, M. M., & Naila-Siddique, L. (2009). Road dust pollution of Cd, Cu, Ni, Pb and Zn along Islamabad Expressway, Pakistan. *Microchemical Journal, 92*(2), 186–192. https://doi.org/10.1016/j.microc.2009.03.009

Fan, P., Lu, X., Yu, B., Fan, X., Wang, L., Lei, K., Yang, Y., Zuo, L., & Rinklebe, J. (2022). Spatial distribution, risk estimation and source apportionment of potentially toxic metal(loid)s in resuspended megacity street dust. *Environment International, 160*, 107073. https://doi.org/10.1016/j.envint.2021.107073

Fdez-Ortiz de Vallejuelo, S., Gredilla, A., da Boit, K., Teixeira, E. C., Sampaio, C. H., Madariaga, J. M., & Silva, L. F. O. (2017). Nanominerals and potentially hazardous elements from coal cleaning rejects of abandoned mines: Environmental impact and risk assessment. *Chemosphere, 169*, 725–733. https://doi.org/10.1016/j.chemosphere.2016.09.125

Ghrefat, H. A., Abu-Rukah, Y., & Rosen, M. A. (2011). Application of geoaccumulation index and enrichment factor for assessing metal contamination in the sediments of Kafrain Dam, Jordan. *Environmental Monitoring and Assessment, 178*(1–4), 95–109. https://doi.org/10.1007/s10661-010-1675-1

Guo, G., Wu, F., Xie, F., & Zhang, R. (2012). Spatial distribution and pollution assessment of heavy metals in urban soils from southwest China. *Journal of Environmental Sciences, 24*(3), 410–418. https://doi.org/10.1016/S1001-0742(11)60762-6

Hakanson, L. (1980). An ecological risk index for aquatic pollution control.a sedimentological approach. *Water Research, 14*(8), 975–1001. https://doi.org/10.1016/0043-1354(80)90143-8

Hassan, A. M. (2017). Mineral composition and geochemistry of the Upper Cretaceous siliciclastics (Nubia Group), Aswan District, south Egypt: Implications for provenance and weathering. *Journal of African Earth Sciences, 135*, 82–95. https://doi.org/10.1016/j.jafrearsci.2017.08.013

Helgen, S. O., & Moore, J. N. (1996). Natural Background Determination and Impact Quantification in Trace Metal-Contaminated River Sediments. *Environmental Science & Technology, 30*(1), 129–135. https://doi.org/10.1021/es950192b

Hu, X., Zhang, Y., Ding, Z., Wang, T., Lian, H., Sun, Y., & Wu, J. (2012). Bioaccessibility and health risk of arsenic and heavy

metals (Cd Co, Cr, Cu, Ni, Pb, Zn and Mn) in TSP and PM2.5 in Nanjing, China. *Atmospheric Environment, 57*, 146–152. https://doi.org/10.1016/j.atmosenv.2012.04.056

Jahanshahi, R., & Zare, M. (2015). Assessment of heavy metals pollution in groundwater of Golgohar iron ore mine area, Iran. *Environmental Earth Sciences, 74*(1), 505–520. https://doi.org/10.1007/s12665-015-4057-8

Jayarathne, A., Egodawatta, P., Ayoko, G. A., & Goonetilleke, A. (2018). Assessment of ecological and human health risks of metals in urban road dust based on geochemical fractionation and potential bioavailability. *Science of the Total Environment, 635*, 1609–1619. https://doi.org/10.1016/j.scitotenv.2018.04.098

Jiang, Y., Shi, L., Guang, A., Mu, Z., Zhan, H., & Wu, Y. (2018). Contamination levels and human health risk assessment of toxic heavy metals in street dust in an industrial city in Northwest China. *Environmental Geochemistry and Health, 40*(5), 2007–2020. https://doi.org/10.1007/s10653-017-0028-1

Jianhua, Q., Xianguo, L., Lijuan, F., & Manping, Z. (2006). Characterization of dust and non-dust aerosols with SEM/EDX. *Journal of Ocean University of China, 5*(1), 85–90. https://doi.org/10.1007/BF02919381

Jose, J., & Srimuruganandam, B. (2020). Investigation of road dust characteristics and its associated health risks from an urban environment. *Environmental Geochemistry and Health, 42*(9), 2819–2840. https://doi.org/10.1007/s10653-020-00521-6

Kabir, Md. H., Kormoker, T., Islam, Md. S., Khan, R., Shammi, R. S., Tusher, T. R., Proshad, R., Islam, M. S., & Idris, A. M. (2021). Potentially toxic elements in street dust from an urban city of a developing country: Ecological and probabilistic health risks assessment. *Environmental Science and Pollution Research, 28*(40), 57126–57148. https://doi.org/10.1007/s11356-021-14581-3

Kamh, S., Khalil, H., Mousa, G., Abdeen, M., & Ghobara, O. (2022). Utilizing Remote Sensing and Lithostratigraphy for Iron and Clay Minerals Mapping in the North of Aswan Area, Egypt. *Delta Journal of Science, 44*(2), 1–16.

Kelepertzis, E., Argyraki, A., & Daftsis, E. (2012). Geochemical signature of surface water and stream sediments of a mineralized drainage basin at NE Chalkidiki, Greece: A pre-mining survey. *Journal of Geochemical Exploration, 114*, 70–81. https://doi.org/10.1016/j.gexplo.2011.12.006

Kim, I.-G., Kim, Y.-B., Kim, R.-H., & Hyon, T.-S. (2021). Spatial distribution, origin and contamination assessment of heavy metals in surface sediments from Jangsong tidal flat, Kangryong river estuary, DPR Korea. *Marine Pollution Bulletin, 168*, 112414. https://doi.org/10.1016/j.marpolbul.2021.112414

Kouchou, A., El Ghachtouli, N., Duplay, J., Ghazi, M., Elsass, F., Thoisy, J. C., Bellarbi, M., Ijjaali, M., & Rais, N. (2020). Evaluation of the environmental and human health risk related to metallic contamination in agricultural soils in the Mediterranean semi-arid area (Saiss plain, Morocco). *Environmental Earth Sciences, 79*(6), 131. https://doi.org/10.1007/s12665-020-8880-1

Kouidri, M., Dali youcef, N., Benabdellah, I., Ghoubali, R., Bernoussi, A., & Lagha, A. (2016). Enrichment and geoaccumulation of heavy metals and risk assessment of sediments from coast of Ain Temouchent (Algeria).

Arabian Journal of Geosciences, 9(5), 354. https://doi.org/10.1007/s12517-016-2377-y

Kowalska, J., Mazurek, R., Gąsiorek, M., Setlak, M., Zaleski, T., & Waroszewski, J. (2016). Soil pollution indices conditioned by medieval metallurgical activity – A case study from Krakow (Poland). *Environmental Pollution, 218*, 1023–1036. https://doi.org/10.1016/j.envpol.2016.08.053

Liang, S., Li, X., Xu, H., Wang, X., & Gao, N. (2013). Spatial-Based Assessment of Heavy Metal Contamination in Agricultural Soils Surrounding a Non-ferrous Metal Smelting Zone. *Bulletin of Environmental Contamination and Toxicology, 91*(5), 526–532. https://doi.org/10.1007/s00128-013-1110-8

Liu, W., Zhao, J., Ouyang, Z., Söderlund, L., & Liu, G. (2005). Impacts of sewage irrigation on heavy metal distribution and contamination in Beijing, China. *Environment International, 31*(6), 805–812. https://doi.org/10.1016/j.envint.2005.05.042

Liu, B., Wang, J., Xu, M., Zhao, L., & Wang, Z. (2019). Spatial distribution, source apportionment and ecological risk assessment of heavy metals in the sediments of Haizhou Bay national ocean park, China. *Marine Pollution Bulletin, 149*, 110651. https://doi.org/10.1016/j.marpolbul.2019.110651

Loska, K., Wiechuła, D., & Korus, I. (2004). Metal contamination of farming soils affected by industry. *Environment International, 30*(2), 159–165. https://doi.org/10.1016/S0160-4120(03)00157-0

Lu, X., Wu, X., Wang, Y., Chen, H., Gao, P., & Fu, Y. (2014). Risk assessment of toxic metals in street dust from a medium-sized industrial city of China. *Ecotoxicology and Environmental Safety, 106*, 154–163. https://doi.org/10.1016/j.ecoenv.2014.04.022

Luo, W., Lu, Y., Giesy, J. P., Wang, T., Shi, Y., Wang, G., & Xing, Y. (2007). Effects of land use on concentrations of metals in surface soils and ecological risk around Guanting Reservoir, China. *Environmental Geochemistry and Health, 29*(6), 459–471. https://doi.org/10.1007/s10653-007-9115-z

Maanan, M., Saddik, M., Maanan, M., Chaibi, M., Assobhei, O., & Zourarah, B. (2015). Environmental and ecological risk assessment of heavy metals in sediments of Nador lagoon, Morocco. *Ecological Indicators, 48*, 616–626. https://doi.org/10.1016/j.ecolind.2014.09.034

Malakootian, M., Mohammadi, A., Nasiri, A., Asadi, A. M. S., Conti, G. O., & Faraji, M. (2021). Spatial distribution and correlations among elements in smaller than 75 μm street dust: Ecological and probabilistic health risk assessment. *Environmental Geochemistry and Health, 43*(1), 567–583. https://doi.org/10.1007/s10653-020-00694-0

Mandeng, E. P. B., Bidjeck, L. M. B., Bessa, A. Z. E., Ntomb, Y. D., Wadjou, J. W., Doumo, E. P. E., & Dieudonné, L. B. (2019). Contamination and risk assessment of heavy metals, and uranium of sediments in two watersheds in Abiete-Toko gold district, Southern Cameroon. *Heliyon, 5*(10), e02591. https://doi.org/10.1016/j.heliyon.2019.e02591

Mazurek, R., Kowalska, J., Gąsiorek, M., Zadrożny, P., Józefowska, A., Zaleski, T., Kępka, W., Tymczuk, M., & Orłowska, K. (2017). Assessment of heavy metals

contamination in surface layers of Roztocze National Park forest soils (SE Poland) by indices of pollution. *Chemosphere, 168*, 839–850. https://doi.org/10.1016/j.chemosphere.2016.10.126

Mekkawi, M. M., ElEmam, A. E., Taha, A. I., Al Deep, M. A., Araffa, S. A. S., Massoud, U. S., & Abbas, A. M. (2021). Integrated geophysical approach in exploration of iron ore deposits in the North-eastern Aswan-Egypt: A case study. *Arabian Journal of Geosciences, 14*(8), 721. https://doi.org/10.1007/s12517-021-06964-0

Meneisy, A. M. (2020). Impact of subsurface structures on groundwater exploration using aeromagnetic and geo-electrical data: A case study at Aswan City, Egypt. *Arabian Journal of Geosciences, 13*(22), 1213. https://doi.org/10.1007/s12517-020-06201-0

Mokhtari, A. R., Feiznia, S., Jafari, M., Tavili, A., Ghaneei-Bafghi, M.-J., Rahmany, F., & Kerry, R. (2018). Investigating the Role of Wind in the Dispersion of Heavy Metals Around Mines in Arid Regions (a Case Study from Kushk Pb–Zn Mine, Bafgh, Iran). *Bulletin of Environmental Contamination and Toxicology, 101*(1), 124–130. https://doi.org/10.1007/s00128-018-2319-3

Mondal, P., de Alcântara Mendes, R., Jonathan, M. P., Biswas, J. K., Murugan, K., & Sarkar, S. K. (2018). Seasonal assessment of trace element contamination in intertidal sediments of the meso-macrotidal Hooghly (Ganges) River Estuary with a note on mercury speciation. *Marine Pollution Bulletin, 127*, 117–130. https://doi.org/10.1016/j.marpolbul.2017.11.041

Moore, J. N., & Langner, H. W. (2012). Can a River Heal Itself? Natural Attenuation of Metal Contamination in River Sediment. *Environmental Science & Technology, 46*(5), 2616–2623. https://doi.org/10.1021/es203810j

Mücke, A. (2000). Environmental conditions in the Late Cretaceous African Tethys: Conclusions from a microscopic-microchemical study of ooidal ironstones from Egypt, Sudan and Nigeria. *Journal of African Earth Sciences, 30*(1), 25–46. https://doi.org/10.1016/S0899-5362(00)00006-3

Muller, G. (1969). Index of geoaccumulation in sediments of the Rhine River. *GeoJournal, 2*, 108–118.

Ngugi, M. R., & Neldner, V. J. (2015). Two-tiered methodology for the assessment and projection of mine vegetation rehabilitation against mine closure restoration goal. *Ecological Management & Restoration, 16*(3), 215–223. https://doi.org/10.1111/emr.12176

Nordstrom, D. K. (2015). Baseline and premining geochemical characterization of mined sites. *Applied Geochemistry, 57*, 17–34. https://doi.org/10.1016/j.apgeochem.2014.12.010

Patinha, C., Durães, N., Sousa, P., Dias, A. C., Reis, A. P., Noack, Y., & Ferreira da Silva, E. (2015). Assessment of the influence of traffic-related particles in urban dust using sequential selective extraction and oral bioaccessibility tests. *Environmental Geochemistry and Health, 37*(4), 707–724. https://doi.org/10.1007/s10653-015-9713-0

Pellinen, V., Cherkashina, T., & Gustaytis, M. (2021). Assessment of metal pollution and subsequent ecological risk in the coastal zone of the Olkhon Island, Lake Baikal, Russia. *Science of The Total Environment,*

786, 147441. https://doi.org/10.1016/j.scitotenv.2021.147441

Pereira, A. A., van Hattum, B., Brouwer, A., van Bodegom, P. M., Rezende, C. E., & Salomons, W. (2008). Effects of iron-ore mining and processing on metal bioavailability in a tropical coastal lagoon. *Journal of Soils and Sediments, 8*(4), 239–252. https://doi.org/10.1007/s11368-008-0017-1

Pérez-López, M., Hermoso de Mendoza, M., López Beceiro, A., & Soler Rodríguez, F. (2008). Heavy metal (Cd, Pb, Zn) and metalloid (As) content in raptor species from Galicia (NW Spain). *Ecotoxicology and Environmental Safety, 70*(1), 154–162. https://doi.org/10.1016/j.ecoenv.2007.04.016

Perret, D., Gaillard, J.-F., Dominik, J., & Atteia, O. (2000). The Diversity of Natural Hydrous Iron Oxides. *Environmental Science & Technology, 34*(17), 3540–3546. https://doi.org/10.1021/es0000089

Proust, D., Fontaine, C., & Dauger, N. (2013). Impacts of weathering and clay mineralogy on heavy metals sorption in sludge-amended soils. *CATENA, 101*, 188–196. https://doi.org/10.1016/j.catena.2012.09.005

Punniyakotti, J., & Ponnusamy, V. (2018). Environmental radiation and potential ecological risk levels in the intertidal zone of southern region of Tamil Nadu coast (HBRAs), India. *Marine Pollution Bulletin, 127*, 377–386. https://doi.org/10.1016/j.marpolbul.2017.11.026

Qingjie, G., Jun, D., Yunchuan, X., Qingfei, W., & Liqiang, Y. (2008). Calculating Pollution Indices by Heavy Metals in Ecological Geochemistry Assessment and a Case Study in Parks of Beijing. *Journal of China University of Geosciences, 19*(3), 230–241. https://doi.org/10.1016/S1002-0705(08)60042-4

Ramasamy, V., Senthil, S., Paramasivam, K., & Suresh, G. (2021). Potential toxicity of heavy metals in beach and intertidal sediments: A comparative study. *Acta Ecologica Sinica, 42*(2), 57–67. https://doi.org/10.1016/j.chnaes.2021.03.006

Romero-Freire, A., Minguez, L., Pelletier, M., Cayer, A., Caillet, C., Devin, S., Gross, E. M., Guérold, F., Pain-Devin, S., Vignati, D. A. L., & Giamberini, L. (2018). Assessment of baseline ecotoxicity of sediments from a prospective mining area enriched in light rare earth elements. *Science of the Total Environment, 612*, 831–839. https://doi.org/10.1016/j.scitotenv.2017.08.128

Sababa, E., & Ekoa Bessa, A. Z. (2022). Heavy Metals Signature in Stream Sediments at Eséka Gold District, Central Africa: A Pre-mining Environmental Assessment. *Chemistry Africa, 5*(2), 413–430. https://doi.org/10.1007/s42250-022-00314-7

Salem, S. M., & El Gammal, E. A. (2015). Iron ore prospection East Aswan, Egypt, using remote sensing techniques. *The Egyptian Journal of Remote Sensing and Space Science, 18*(2), 195–206. https://doi.org/10.1016/j.ejrs.2015.04.003

Shahmoradi, B., Hajimirzaei, S., Amanollahi, J., Wantalla, K., Maleki, A., Lee, S.-M., & Shim, M. J. (2020). Influence of iron mining activity on heavy metal contamination in the sediments of the Aqyazi River, Iran. *Environmental Monitoring and Assessment, 192*(8), 521. https://doi.org/10.1007/s10661-020-08466-0

Shaltout, A. A., Gomma, M. M., & Ali-Bik, M. W. (2012). Utilization of standardless analysis algorithms using WDXRF and XRD for Egyptian iron ore identification: Standardless analysis of Egyptian iron ores. *X-Ray Spectrometry, 41*(6), 355–362. https://doi.org/10.1002/xrs.2410

Shen, Q., Demisie, W., Zhang, S., & Zhang, M. (2020). The Association of Heavy Metals with Iron Oxides in the Aggregates of Naturally Enriched Soil. *Bulletin of Environmental Contamination and Toxicology, 104*(1), 144–148. https://doi.org/10.1007/s00128-019-02739-2

Shirani, M., Afzali, K. N., Jahan, S., Strezov, V., & Soleimani-Sardo, M. (2020). Pollution and contamination assessment of heavy metals in the sediments of Jazmurian playa in southeast Iran. *Scientific Reports, 10*(1), 4775. https://doi.org/10.1038/s41598-020-61838-x

Singh, H., Pandey, R., Singh, S. K., & Shukla, D. N. (2017). Assessment of heavy metal contamination in the sediment of the River Ghaghara, a major tributary of the River Ganga in Northern India. *Applied Water Science, 7*(7), 4133–4149. https://doi.org/10.1007/s13201-017-0572-y

Soliman, M. A., Habib, M. E., & Ahmed, E. A. (1986). Sedimentologic and tectonic evolution of the Upper Cretaceous-Lower Tertiary succession at Wadi Qena, Egypt. *Sedimentary Geology, 46*(1–2), 111–133. https://doi.org/10.1016/0037-0738(86)90009-6

Sundar, S., Roy, P. D., Chokkalingam, L., & Ramasamy, N. (2021). Evaluation of metals and trace elements in sediments of Kanyakumari beach (southernmost India) and their possible impact on coastal aquifers. *Marine Pollution Bulletin, 169*, 112527. https://doi.org/10.1016/j.marpolbul.2021.112527

Suresh, G., Ramasamy, V., & Meenakshisundaram, V. (2012). Effect of lower grain sized particles on natural radiation level of the Ponnaiyar river sediments. *Applied Radiation and Isotopes, 70*(3), 556–562. https://doi.org/10.1016/j.apradiso.2011.11.048

Suryawanshi, P. V., Rajaram, B. S., Bhanarkar, A. D., & Chalapati-Rao, C. V. (2016). Determining heavy metal contamination of road dust in Delhi, India. *Atmósfera*. https://doi.org/10.20937/ATM.2016.29.03.04

Taylor, D. (1971). An outline of the geology of the Bukit Ibam orebody, Rompin, Pahang. *Bulletin of the Geological Society of Malaysia, 4*, 71–89. https://doi.org/10.7186/bgsm04197105

Taylor, S. R. (1964). Abundance of chemical elements in the continental crust: A new table. *Geochimica Et Cosmochimica Acta, 28*(8), 1273–1285. https://doi.org/10.1016/0016-7037(64)90129-2

Taylor, R. M. (1968). THE ASSOCIATION OF MANGANESE AND COBALT IN SOILS-FURTHER OBSERVATIONS. *Journal of Soil Science, 19*(1), 77–80. https://doi.org/10.1111/j.1365-2389.1968.tb01522.x

Tomlinson, D. L., Wilson, J. G., Harris, C. R., & Jeffrey, D. W. (1980). Problems in the assessment of heavy-metal levels in estuaries and the formation of a pollution index. *Helgoländer Meeresuntersuchungen, 33*(1–4), 566–575. https://doi.org/10.1007/BF02414780

Turekian, K. K., & Wedepohl, K. H. (1961). Distribution of the Elements in Some Major Units of the Earth's Crust. *Geological Society of America Bulletin, 72*(2), 175. https://doi.org/10.1130/0016-7606(1961)72[175:DOTEIS]2.0.CO;2

Turner, A. (2019). Lead pollution of coastal sediments by ceramic waste. *Marine Pollution Bulletin, 138*, 171–176. https://doi.org/10.1016/j.marpolbul.2018.11.013

USEPA. (2002). *Guidance for Comparing Background and Chemical Concentrations in Soil for CERCLA Sites* (EPA 540-R-01-003). Office of Emergency and Remedial Response, U.S. Environmental Protection Agency, Washington, DC.

Varol, M. (2011). Assessment of heavy metal contamination in sediments of the Tigris River (Turkey) using pollution indices and multivariate statistical techniques. *Journal of Hazardous Materials, 195*, 355–364. https://doi.org/10.1016/j.jhazmat.2011.08.051

Viana, M., Kuhlbusch, T. A. J., Querol, X., Alastuey, A., Harrison, R. M., Hopke, P. K., Winiwarter, W., Vallius, M., Szidat, S., Prévôt, A. S. H., Hueglin, C., Bloemen, H., Wåhlin, P., Vecchi, R., Miranda, A. I., Kasper-Giebl, A., Maenhaut, W., & Hitzenberger, R. (2008). Source apportionment of particulate matter in Europe: A review of methods and results. *Journal of Aerosol Science, 39*(10), 827–849. https://doi.org/10.1016/j.jaerosci.2008.05.007

Wang, X., & Li, Y. (2011). Measurement of Cu and Zn adsorption onto surficial sediment components: New evidence for less importance of clay minerals. *Journal of Hazardous Materials, 189*(3), 719–723. https://doi.org/10.1016/j.jhazmat.2011.03.045

Wang, P., Xue, J., & Zhu, Z. (2021). Comparison of heavy metal bioaccessibility between street dust and beach sediment: Particle size effect and environmental magnetism response. *Science of The Total Environment, 777*, 146081. https://doi.org/10.1016/j.scitotenv.2021.146081

Wedepohl, K. H. (1995). The composition of the continental crust. *Geochimicaet Cosmochimica Acta, 59*(7), 1217–1232.

Weissmannová, H. D., & Pavlovský, J. (2017). Indices of soil contamination by heavy metals – methodology of calculation for pollution assessment (minireview). *Environmental Monitoring and Assessment, 189*(12), 616. https://doi.org/10.1007/s10661-017-6340-5

Williams, J. A., & Antoine, J. (2020). Evaluation of the elemental pollution status of Jamaican surface sediments using enrichment factor, geoaccumulation index, ecological risk and potential ecological risk index. *Marine Pollution Bulletin, 157*, 111288. https://doi.org/10.1016/j.marpolbul.2020.111288

Wu, W., Wu, P., Yang, F., Sun, D., Zhang, D.-X., & Zhou, Y.-K. (2018). Assessment of heavy metal pollution and human health risks in urban soils around an electronics manufacturing facility. *Science of the Total Environment, 630*, 53–61. https://doi.org/10.1016/j.scitotenv.2018.02.183

Yalcin, M. G., Coskun, B., Nyamsari, D. G., & Yalcin, F. (2019). Geomedical, ecological risk, and statistical assessment of hazardous elements in shore sediments of the Iskenderun Gulf, Eastern Mediterranean, Turkey. *Environmental Earth Sciences, 78*(15), 438. https://doi.org/10.1007/s12665-019-8435-5

Yang, Y.-Y., Wu, H.-N., Shen, S.-L., Horpibulsuk, S., Xu, Y.-S., & Zhou, Q.-H. (2014). Environmental impacts caused by phosphate mining and ecological restoration: A case history in Kunming, China. *Natural Hazards, 74*(2), 755–770. https://doi.org/10.1007/s11069-014-1212-6

Yesilkanat, C. M., & Kobya, Y. (2021). Spatial characteristics of ecological and health risks of toxic heavy metal pollution from road dust in the Black Sea coast of Turkey. *Geoderma Regional, 25*, e00388. https://doi.org/10.1016/j.geodrs.2021.e00388

Youssef, M. A. A., Abd El-Gawad, A. M. S., & Farag, K. S. I. (2018). Iron ore prospecting based on very low frequency-electromagnetic and geoelectrical resistivity at Wadi Abu Subeira, Northeastern Aswan, South Egypt. *NRIAG Journal of Astronomy and Geophysics, 7*(2), 253–263. https://doi.org/10.1016/j.nrjag.2018.08.002

Zhao, W., Gu, C., Ying, H., Feng, X., Zhu, M., Wang, M., Tan, W., & Wang, X. (2021). Fraction distribution of heavy metals and its relationship with iron in polluted farmland soils around distinct mining areas. *Applied Geochemistry, 130*, 104969. https://doi.org/10.1016/j.apgeochem.2021.104969

Zhiyuan, W., Dengfeng, W., Huiping, Z., & Zhiping, Q. (2011). Assessment of Soil Heavy Metal Pollution with Principal Component Analysis and Geoaccumulation Index. *Procedia Environmental Sciences, 10*, 1946–1952. https://doi.org/10.1016/j.proenv.2011.09.305